

Effect of ablated particle flux on MgO nanowire growth by pulsed laser deposition

Aurelian Marcu

Institute of Scientific and Industrial Research, Osaka University, 8-1 Mihogaoka, Ibaraki, Osaka 567-0047, Japan and National Institute of Laser Plasma and Radiation Physics, Laser Department, P.O. Box MG-36, Atomistilor 409, Bucharest-Magurele, Romania

Takeshi Yanagida,^{a)} Kazuki Nagashima, Hidekazu Tanaka, and Tomoji Kawai

Institute of Scientific and Industrial Research, Osaka University, 8-1 Mihogaoka, Ibaraki, Osaka 567-0047, Japan

(Received 1 May 2007; accepted 21 May 2007; published online 2 July 2007)

Oxide nanowire growth using a pulsed laser deposition (PLD) is a promising process since this essentially allows incorporating a rich functionality of various transition metal oxides into nanowires via the heterostructures. Here we investigate the effect of ablated particle flux on magnesium oxide nanowire growth by PLD. When varying the distance between the ablated material and the substrate, the small variation in ablated particle flux generated by a different plume expansion time influences mainly the growth rate while keeping the growth regime. However, varying the laser energy changes not only the growth rate but also the growth regime. Below a critical value of the laser energy the surface morphology tends to show an island growth rather than a nanowire growth. We attribute the existence of such a threshold to the desorption process from the catalyst droplet. © 2007 American Institute of Physics. [DOI: 10.1063/1.2751077]

One-dimensional nanostructures including nanowires have become the subject of extensive research due to their great potential for fundamental studies and applications in nanoscale science and engineering.^{1–7} Since oxides are well known to exhibit a rich variety of physical properties including ferromagnetism, ferroelectric, and superconducting,^{8–10} the availability of various oxide nanowires and the heterostructures might add further functionalities to nanowire-based devices. Magnesium oxide (MgO) has been used as a versatile single crystal substrate for oxide thin film growth due to the small lattice mismatch with various functional transition metal oxides.^{9,10} Therefore, the feasibility of MgO nanowires allows us to incorporate desired transition metal oxides into the oxide nanowires via the heterostructures.^{11–13} Since the interface of oxide heterostructures plays an important role on the properties,¹⁴ the *in situ* construction of oxide heterostructures in oxide nanowires is strongly desired to prevent interface degradations due to atmospheric exposure. As to the synthesis of oxide materials, pulsed laser deposition (PLD) has been one of the most powerful techniques to fabricate various oxide thin films,^{15,16} nonequilibrium oxides,¹⁷ and the heterostructures.¹⁸ Thus, the feasibility of PLD technique to fabricate MgO nanowires would enable us to integrate rich functionalities of oxides into nanowires via *in situ* construction of oxide heterostructures. In PLD the ablated particle flux is well known to play an important role on the synthesis of well-defined oxides including the crystallinity, the stoichiometry, and so on.^{19–21} However, the knowledge regarding the effect of ablated particle flux on oxide nanowire growth by PLD is still scarce.²² Here we investi-

gate the effect of ablated particle flux on MgO nanowire growth using PLD.

MgO nanowires were grown on MgO (100) single crystal substrate by Au catalyst-assisted PLD technique. Prior to the nanowire growth, Au catalysts were sputtered on the 5 mm × 5 mm MgO single crystal substrate. The background pressure of the PLD chamber was set to be 10⁻⁴ Pa. An ArF excimer laser (Lamda-Physik COMPex 102, λ = 193 nm) was used for the laser ablation by varying the pulse repetition rate *f* from 3 to 10 Hz and the laser energy *P_l* from 10 to 80 mJ. MgO single crystals were used as source of ablation plume during the nanowire growth. The distance between the substrate and the target *D_{st}* was varied from 25 to 50 mm. Oxygen gas was introduced into the chamber at the constant ambient pressure of 10 Pa. Prior to the laser ablation, the Au-coated MgO (100) substrate was preheated at 820 °C and kept for 10 min. After the deposition, the samples were cooled down to room temperature within 30 min. The nanowire morphology was characterized by field emission scanning electron microscopy (FESEM) (JEOL JSM-6330FT) at an accelerating voltage of 30 kV. The length of MgO nanowires was analyzed by calculating the average for 500 samples in FESEM images for statistical reliability. High-resolution transmission electron microscopy (HRTEM) (JEOL JEM-3000F) coupled with energy dispersive spectroscopy was used to evaluate the diameter, the crystallinity and the composition of the fabricated nanowires. Samples for TEM were prepared by placing a drop of the sample suspension on a copper microgrid (JEOL 7801–11613). TEM measurements were performed at the accelerating voltage of 300 kV.

Figure 1(a) shows the FESEM image of fabricated MgO nanowires. The nanowires were grown at *D_{st}* = 35 mm, *P_l*

^{a)}Electronic mail: yanagi32@sanken.osaka-u.ac.jp

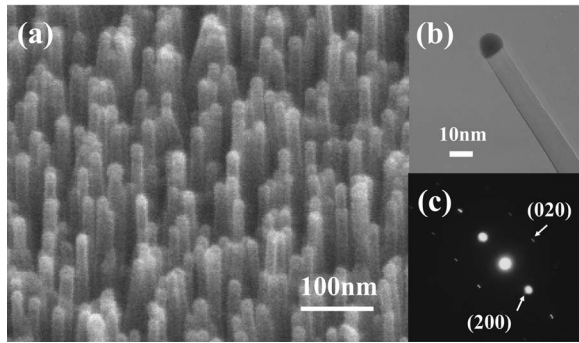


FIG. 1. (a) FESEM images of MgO nanowires grown on MgO (100) single crystal substrate. (b) HRTEM image of MgO nanowires. (c) SAED pattern in HRTEM image. MgO nanowires were grown at $D_{st}=35$ mm, $P_l=40$ mJ, and $f=10$ Hz for 60 min.

$=40$ mJ, and $f=10$ Hz for 60 min. It can be seen that nanowires are epitaxially grown on MgO (100) single crystal. The single crystal nature can be also seen in the HRTEM image [Fig. 1(b)] and the selected area electron diffraction (SAED) pattern [Fig. 1(c)]. When varying D_{st} from 25 to 50 mm the major change was found to be the nanowire length. The diameter maintained almost constant during growth within the investigated time scale, 60 min. Figure 2 shows the variation of nanowire length h when varying D_{st} . The nanowires were grown at $P_l=40$ mJ and $f=10$ Hz for 60 min. Increasing D_{st} resulted in decreasing the nanowire length. This trend can be interpreted in terms of the variation of ablated particle flux via the different plume expansion time. The number of ablated atoms inside the plume should roughly be the same while the plume expands at different distances although their speeds and respectively average kinetic energies would slightly change. Here we assume a standard radius exponential variation model for the plume radial expansion.²³ Considering that the substrate surface is visible under a different solid angle from the laser irradiated area, the relationship between the substrate subtended area (S_s) and the total plume front area (S_{tot}) can be estimated by the formula- $S_s=S_{tot}\{1-\cos[\arctan(L/2D_{st})]\}$, where L is the width of the

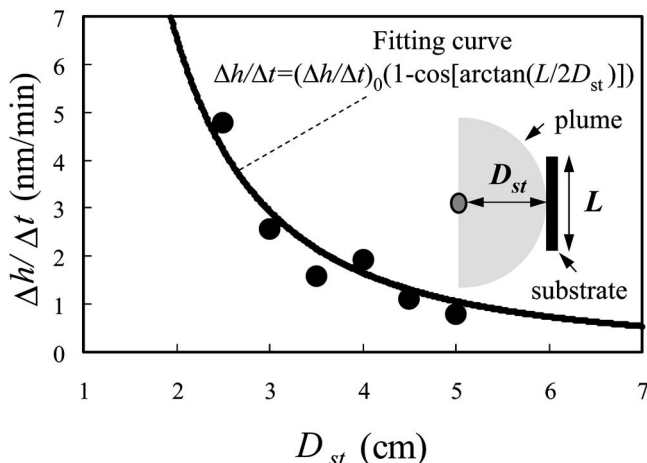


FIG. 2. Relationship between the nanowire growth rate $\Delta h/\Delta t$ and the target-substrate distance D_{st} . The calculated model curve is shown in the figure for comparison. The nanowires were grown for 60 min. The inset shows the schematic illustration of the model and the notation.

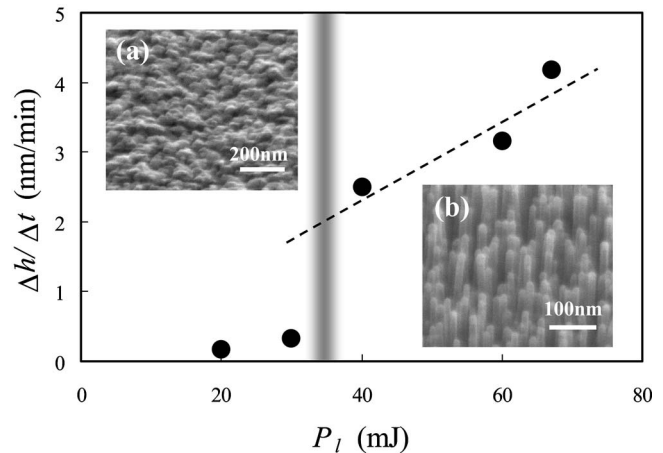


FIG. 3. Effect of laser energy P_l on the nanowire growth rate $\Delta h/\Delta t$. The insets show FESEM images of nanowires grown at 20 and 40 mJ of P_l .

substrate. By assuming the ablated particles with a quasiuniform radial distribution, the number of ablated particles arriving on the substrate surface should change in proportion to the plume front surface variation: $N_s=N_{tot}\{1-\cos[\arctan(L/2D_{st})]\}$, where N_s and N_{tot} are the number of ablated particles arriving on the substrate surface and the total number of ablated particles, respectively. Furthermore, we approximate that the ablated particles that arrived on the surface mostly contribute to the nanowire formation. Using these approximations, the relationship between the nanowire growth rate $\Delta h/\Delta t$ and D_{st} can be approximated to $\Delta h/\Delta t=(\Delta h/\Delta t)_0\{1-\cos[\arctan(L/2D_{st})]\}$, where $(\Delta h/\Delta t)_0$ is the nanowire growth rate when all the ablated particles are deposited on the substrate. The fitting curve using this formula is shown in Fig. 2. The excellent agreement between the model and the experimental data can be seen. This clearly indicates that the plume expansion phenomenon when increasing D_{st} governs the variation in the nanowire length via the decreased number of ablated particle flux. In other words, the variation in D_{st} does not affect the growth regime of nanowires within the investigated range.

Figure 3 shows the effect of laser energy P_l on the nanowire growth rate $\Delta h/\Delta t$. The nanowires were deposited at $D_{st}=35$ mm and $f=10$ Hz for 60 min. Below 20 mJ there was no ablation phenomenon in our experiments, which is indeed in good agreement with the trend of previous investigation in the context with MgO thin film formation.²⁴ A proportional relationship between $\Delta h/\Delta t$ and P_l was found above 40 mJ. This is solely due to the variation in the ablated particle flux. However, below 40 mJ the surface morphology tends to show an island growth rather than a nanowire growth, as shown in the inset FESEM images. It is noted that the absence of nanowire growth for low P_l range was found even for a three times longer deposition time—180 min. This indicates that the number of ablated particles per unit time rather than the total number of ablated particles is critical for the nanowire growth. When decreasing the repetition rate from 10 to 3 Hz, it was found that there was no significant influence on the nanowire morphology as long as P_l was set to be above 40 mJ. These experimental results highlight the existence of a threshold of P_l for the MgO nanowire growth.

Within the framework of vapor-liquid-solid (VLS) mechanism, a supersaturation within catalyst droplets is an important process.²⁵⁻²⁷ In other words, the Mg concentration inside the Au catalyst droplet has to reach the critical concentration by incorporating the diffused adatoms. Note that the adatoms diffused from surroundings into the catalyst rather than the direct impinging flux dominates the VLS nanowire growth.²⁷

In fact, the variation of P_l changes mainly the number of adatoms on the substrate surface, which contribute to such Mg incorporation into the catalyst droplet. Since the ambient temperature and the oxygen pressure were set to be constant in this series of experiments, the critical concentration and the diffusion length of adatoms are assumed to be constant. In general, the desorption of Mg species from the Au catalyst droplet exists.²⁷ In the presence of such desorption, the accumulated Mg species within the catalyst, which are supplied from outside, must compensate the amount of Mg concentration consumed by the desorption. When the ablated particle flux is not enough to compensate such decreasing of Mg concentration due to the desorption, VLS nanowire growth might be no longer possible. This simple scenario seems to be able to explain the experimental trend when varying P_l . The ablated particle flux decreases with decreasing P_l , as also demonstrated by MgO thin film formation study.²⁵ However, as mentioned earlier, in the lower P_l range between 20 and 40 mJ, in which the ablated particle flux still exists, the surface morphology tends to show an island growth rather than a nanowire growth. Thus, the presence of the desorption process must be considered in order to explain the threshold of P_l in terms of the competition between the desorption process and the number of incoming adatoms into the catalyst droplet. Although this scenario must be applicable to the plume expansion phenomenon when varying D_{st} , the effect of P_l on the ablated particle flux seems to be much stronger than the variation of D_{st} in terms of the ablated particle flux within the investigated range. These experimental results highlight the crucial role of the ablated particle flux and the competition with the desorption process on MgO nanowire growth using catalyst-assisted PLD.

In summary, we have shown the effect of ablated particle flux on MgO nanowire growth by PLD. The variation in ablated particle flux generated by a different plume expansion time, when varying the distance between the target and the substrate, influences mainly the growth rate while keeping the growth regime. However, the variation of the laser energy influences not only the growth rate but also the growth regime. Below a critical value of the laser energy the surface morphology tends to show an island growth rather than a nanowire growth. We attribute the existence of such a threshold to the desorption process from the catalyst droplet.

The authors would like to thank the Ministry of Education, Culture, Sports, Science and Technology of Japan for funding and supporting this project through the Center of Excellence (COE) program. The authors also acknowledge M. Kanai for constructive advices and T. Ishibashi for his invaluable technical supports.

- ¹F. Patolsky, B. D. Timko, G. Yu, Y. Fang, A. B. Greytak, G. Zheng, and C. M. Lieber, *Science* **313**, 1100 (2006).
- ²J. Xiang, W. Lu, Y. Hu, Y. Wu, H. Yan, and C. M. Lieber, *Nature (London)* **441**, 489 (2006).
- ³R. S. Friedman, M. C. McAlpine, D. S. Ricketts, D. Ham, and C. M. Lieber, *Nature (London)* **434**, 1085 (2005).
- ⁴O. Hayden, R. Agarwal, and C. M. Lieber, *Nat. Mater.* **5**, 352 (2006).
- ⁵F. Patolsky, G. Zheng, and C. M. Lieber, *Anal. Chem.* **78**, 4260 (2006).
- ⁶G. Zheng, F. Patolsky, Y. Cui, W. U. Wang, and C. M. Lieber, *Nat. Biotechnol.* **23**, 1294 (2005).
- ⁷C. J. Barrelet, J. Bao, M. Lončar, H. G. Park, F. Capasso, and C. M. Lieber, *Nano Lett.* **6**, 11 (2006).
- ⁸H. Tian, Y. Wang, D. Wang, J. Miao, J. Qi, H. L. W. Chan, and C. L. Choy, *Appl. Phys. Lett.* **89**, 142905 (2006).
- ⁹M. Ishikawa, H. Tanaka, and T. Kawai, *Appl. Phys. Lett.* **86**, 222504 (2005).
- ¹⁰M. I. Faley, S. B. Mi, A. Petraru, C. L. Jia, U. Poppe, and K. Urban, *Appl. Phys. Lett.* **89**, 082507 (2006).
- ¹¹B. Lei, C. Li, D. Zhang, S. Han, and C. Zhou, *J. Phys. Chem. B* **109**, 18799 (2005).
- ¹²Z. Li, D. Zhang, S. Han, C. Li, B. Lei, W. Lu, J. Fang, and C. Zhou, *J. Am. Chem. Soc.* **127**, 6 (2005).
- ¹³D. Zhang, Z. Liu, S. Han, C. Li, B. Lei, M. P. Stewart, J. M. Tour, and C. Zhou, *Nano Lett.* **4**, 2151 (2004).
- ¹⁴K. Nagashima, T. Yanagida, H. Tanaka, and T. Kawai, *J. Appl. Phys.* **101**, 026103 (2007).
- ¹⁵T. Kanki, T. Yanagida, B. Vilquin, H. Tanaka, and T. Kawai, *Phys. Rev. B* **71**, 012403 (2005).
- ¹⁶T. Yanagida, H. Tanaka, T. Kawai, E. Ikenaga, M. Kobata, J. J. Kim, and K. Kobayashi, *Phys. Rev. B* **73**, 132503 (2006).
- ¹⁷H. Ryoken, N. Ohashi, I. Sakaguchi, Y. Adachi, S. Hishita, and H. Haneda, *J. Cryst. Growth* **287**, 134 (2006).
- ¹⁸T. Kanki, Y. G. Park, H. Tanaka, and T. Kawai, *Appl. Phys. Lett.* **283**, 4860 (2003).
- ¹⁹T. Yanagida, T. Kanki, B. Vilquin, H. Tanaka, and T. Kawai, *Phys. Rev. B* **70**, 184437 (2004).
- ²⁰T. Yanagida, T. Kanki, B. Vilquin, H. Tanaka, and T. Kawai, *J. Appl. Phys.* **97**, 033905 (2005).
- ²¹T. Yanagida, T. Kanki, B. Vilquin, H. Tanaka, and T. Kawai, *J. Appl. Phys.* **99**, 053908 (2006).
- ²²M. Lorenz, E. M. Kaidashev, A. Rahm, Th. Nobis, J. Lenzner, G. Wagner, D. Spemann, H. Hochmuth, and M. Grundmann, *Appl. Phys. Lett.* **86**, 143113 (2005).
- ²³E. V. Pechen, A. V. Varlashkin, S. I. Kranosvobodtsev, B. Brunner, and K. F. Renk, *Appl. Phys. Lett.* **66**, 2292 (1995).
- ²⁴D. J. Lichtenwalner, O. Auciello, R. Dat, and A. I. Kingon, *J. Appl. Phys.* **74**, 7497 (1993).
- ²⁵R. S. Wagner and W. C. Ellis, *Trans. Metall. Soc. AIME* **233**, 1052 (1965).
- ²⁶J. B. Hannon, S. Kodambaka, F. M. Ross, and R. M. Tromp, *Nature (London)* **440**, 69 (2006).
- ²⁷V. G. Dubrovskii, N. V. Sibirev, G. E. Cirilin, J. C. Harmand, and V. M. Ustinov, *Phys. Rev. E* **73**, 021603 (2006).